Electroluminescence from Er-doped Si-rich silicon nitride light emitting diodes

S. Yerci,[1] R. Li,[1] and L. Dal Negro[1,2,a)]

[1]*Department of Electrical and Computer Engineering, Boston University, 8 Saint Mary's street, Boston, Massachusetts 02215-2421, USA*
[2]*Photonics Center, Boston University, 8 Saint Mary's street, Boston, Massachusetts 02215-2421, USA and Division of Materials Science and Engineering, Boston University, 15 Saint Mary's street, Brookline, Massachusetts 02446, USA*

Electrical devices based on Erbium (Er) doping of silicon nitride have been fabricated by reactive cosputtering and intense, room temperature Er electroluminescence was observed in the visible (527, 550, and 660 nm) and near-infrared (980 and 1535 nm) spectral ranges at low injection voltages (<5 V EL turn on). The electrical transport mechanism in these devices was investigated and the excitation cross section for the 1535 nm Er emission was measured under electrical pumping, resulting in a value (1.2×10^{-15} cm^2) comparable to optical pumping. These results indicate that Er-doped silicon nitride has a large potential for the engineering of light sources compatible with Si technology. © 2010 American Institute of Physics. [doi:10.1063/1.3483771]

Silicon (Si) photonics has attracted a vast amount of attention since it can provide a cost-effective solution for the monolithic integration of electronic and optical technologies on the same Si chip. One of the major challenges of Si photonics is the realization of efficient light sources using materials compatible with the Si technology.[1] Light emitting diodes (LEDs) made of erbium (Er)-doped crystalline Si and Si nanocrystals embedded in SiO$_2$ (Er:SiO$_x$) operating at the telecom wavelength of 1535 nm have been reported in the literature.[2–6] However, these devices are limited by either strong temperature quenching due to efficient energy back-transfer in Si (Ref. 2) or by the difficulty in engineering stable and efficient electrical injection in SiO$_x$-based dielectrics.[3–6] Alternatively, silicon nitride materials (SiN$_x$) possess lower band gaps and larger density of trap states near midgaps, defining an alternative approach for the development of efficient Si-based LEDs capable of stable operation at low injection voltages.[7,8] Based on this approach, we have recently shown that Er:SiN$_x$ has several advantages over Er:SiO$_x$ due to a very efficient energy coupling to Er ions,[9] a larger refractive index which enables integration with compact photonic and plasmonic nanostructures,[10–14] and lower free carrier absorption losses at 1535 nm.[10] Finally, LEDs based on amorphous-Si/silicon nitride superlattice structures emitting in the visible and near-infrared spectral ranges and operating at voltages as low as 6 V have been recently demonstrated.[15]

In this paper, we investigate room temperature Er electroluminescence (EL) in the visible and near-infrared spectral ranges and we demonstrate 1535 nm Er emission under low injection voltages (<5 V EL turn on). Additionally, we investigate the nature of electrical transport and measure the effective Er excitation cross section at 1535 nm in Er:SiN$_x$ devices under electrical pumping.

Er:SiN$_x$ films (approximately 50 nm thick) with an excess Si atomic concentrations (Si at. %) ranges between 5.0% and 10.5% and Er at. % of $\sim$2.5 were deposited on p-type Si (100) substrates (resistance of 0.1–1 Ω cm) using N$_2$ reactive rf-magnetron cosputtering from Si and Er targets. The details of the fabrication parameters can be found in Ref. 16. The samples were postannealed in a rapid thermal annealing furnace at 1000 °C for 200 s under N$_2$ atmosphere. Aluminum (Al) was deposited to the back side of Si substrate and annealed at 550 °C to form Ohmic contact. Indium tin oxide (ITO) layer of $\sim$30 nm was deposited on Er:SiN$_x$ as n-type top electrode using rf-magnetron sputtering onto 1 mm^2 (or 0.1 mm^2) circular areas defined by standard photolithography. Finally, a ring-shaped Al top contact was deposited on ITO by a second step of photolithography.
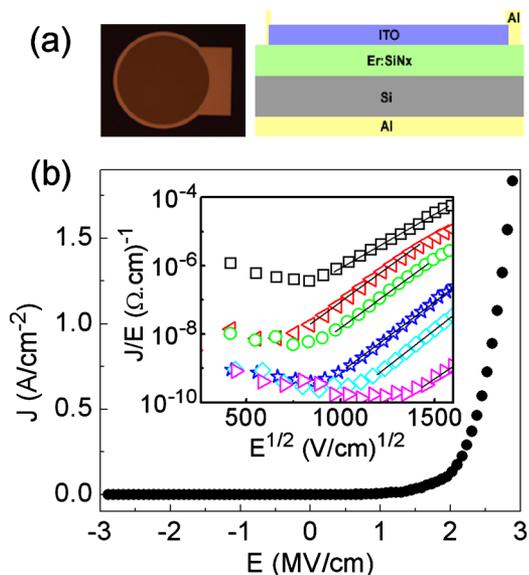
FIG. 1. (Color online) (a) A top image and a schematic cross section view of the Er:SiN$_x$ LED. (b) Current density J vs electric field E plot of the device used in the EL measurements. Inset shows the J/E vs E$^{1/2}$ plot of the samples with an Er at. % of $\sim$2.5 and excess Si at. % of 5.0 (right triangles), 6.0 (diamonds), 6.5 (stars), 7.5 (circles), 8.5 (left triangles), and 10.5 (squares). Straight lines are guide to the eye. 2/3 of the collected data points are skipped for clarity.

a)Author to whom correspondence should be addressed. Electronic mail: dalnegro@bu.edu.
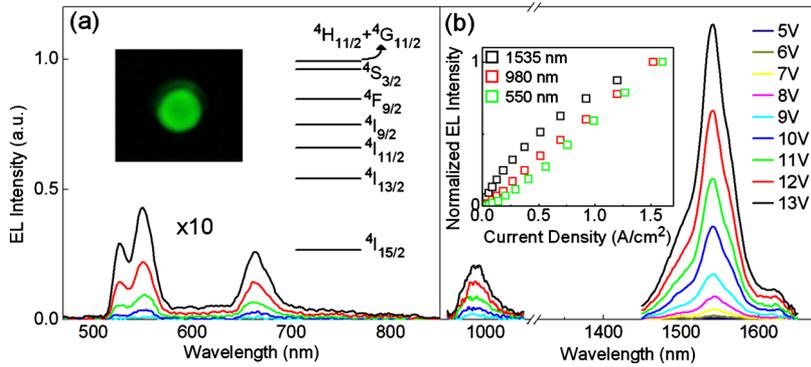
FIG. 2. (Color online) (a) The visible EL spectra of Er:SiN$_x$ LED [multiplied by 10 compared to the data given in part (b)] at voltages between 9 and 13 V. In the inset: image of the emitting surface with an area of 1 mm^2 and schematic representation of Er energy levels. (b) The infrared EL spectra of Er:SiN$_x$ LED at various voltages. In the inset: the current density dependencies of the EL intensities of peaks centered at 550, 980, and 1535 nm (The current dependence of the EL intensity of the peak at 660 nm is almost identical to the one at 550 nm and therefore it is not shown for clarity).

A top view (taken by a charge coupled device camera) and a schematic cross sectional view of the device are shown in Fig. 1(a). Current-voltage characteristics of the samples were measured using a Keithley 2400-LV SourceMeter. The EL spectra of the devices were measured using an extended photomultiplier tube (Hamamatsu R5509-73) detector attached to a monochromator (Oriel 74100). Time-resolved EL were excited using an HP 214A pulse generator and the EL traces were directly detected using an oscilloscope (Agilent 54622A) coupled to the photomultiplier tube detector. Current passing through the devices were measured using a current transformer attached to the oscilloscope.

In Fig. 1(b) we show the variation in current density (J) with the applied electric field (E) for the device used in the EL experiments. This data show a rectifying behavior which is consistent, within the range of electric fields considered for the EL experiments, with a Poole–Frenkel (PF) emission mechanism. According to this model,[17] the current density divided (J) by the electric field (E) shows a linear dependence with respect to E$^{1/2}$, as shown in the inset of Fig. 1(b), and follows the equation $J \propto E \exp[-q(\phi_B - \sqrt{qE/\pi\varepsilon})/k_BT]$ where q is the elementary charge, ϕ_B is the voltage barrier, ε is the dynamic permittivity, k_B is the Boltzmann constant and T is the temperature. Moreover, we show in the inset of Fig. 1(b) that the conductivity of the devices increases with the excess Si in the films, as a result of an increased density of trap states in the SiN$_x$ band gap.[4,7] Consistently, it was recently shown that the PF barrier height also decreases by increasing the excess Si, thus leading to a larger probability for the PF trap emission.[18]

Under electrical pumping, our device structures exhibit several EL bands; 527 nm, 550 nm, 660 nm, 980 nm, and 1535 nm which are assigned to the transitions of Er ions from the excited energy states $^4F_{7/2}$, $^2H_{11/2}$, $^4S_{9/2}$, $^4I_{11/2}$, and $^4I_{13/2}$ to the ground state ($^4I_{15/2}$), respectively, as sketched in the inset of Fig. 2(a).[5] An optical image of the visible Er emission collected from the active area by a standard camera (Canon Rebel XTi) is shown in the inset of Fig. 2(a). This emission, which can easily be seen by naked eye, was found to be stable over time and spatially homogeneous across the entire active area of the device. The 1535 nm Er EL, shown in Fig. 2(b), was measured at voltages as low as 5 V, while all the other bands were detectable at voltages larger than 8 V.[19] It should be noted that a 5 V turn on voltage for the 1535 nm EL of Er:SiN$_x$ is smaller than what previously reported for Er:SiO$_x$ devices,[3,5] and it is very significant for the future integration of Er:SiN$_x$ devices with the existing Si technology. The intensities of 550 and 660 nm peaks are approximately eight times smaller compared to 980 nm peak

as shown in Fig. 2. The integrated EL intensity of the 550 and 980 nm band increases linearly while that of 1535 nm shows a slight sublinear behavior at high injection current density, as shown in the inset of Fig. 2(b), due to the onset of upconversion processes from the Er $^4I_{13/2}$ energy state.[20] The quantification of Er upconversion phenomena under electrical excitation is currently in progress in this materials platform.

In order to quantify the efficiency of Er excitation under electrical pumping, we calculate the electrical excitation cross section (σ) of the Er 1535 nm EL band by measuring the time response of the EL intensity (EL rise time) at different excitation current densities.[16] Four representative rise & decay traces of Er EL measured under different excitation conditions (voltages) are shown in the inset of Fig. 3. We notice that the EL decay time of Er at 1535 nm does not sensibly depend on injection conditions while the EL rise time significantly depends on the injected electron flux (Fig. 3, inset). Therefore, under our injection conditions Er excitation occurs in the linear regime without significant contributions from upconversion processes, and we can use the well-known expression $1/\tau_{on} = \sigma\phi + 1/\tau_{off}$ to extract, by a linear fit, the electrical excitation cross section of the Er 1535 nm emission.[16] In Fig. 3 we plot the inverse rise time for the 1535 nm Er EL as a function of the carrier flux along with the linear fit to this data. In this particular device, the Er excitation cross section at 1535 nm under electrical pumping was found to be 1.2×10^{-15} cm^2, which is comparable to what was observed under optical excitation and much larger than the values reported for Er doped crystalline Si diodes operating in the impact excitation regime.[21]
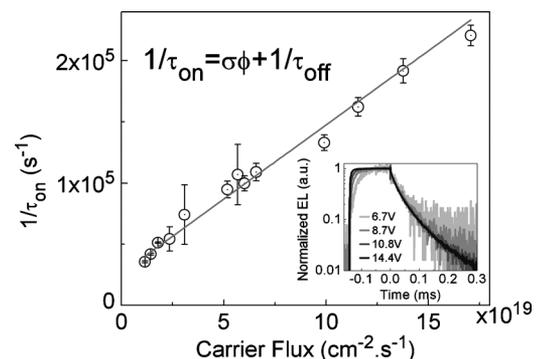
FIG. 3. Inverse rise time ($1/\tau_{on}$) of the EL of the Er:SiN$_x$ LED vs the carrier flux (ϕ) measured at room temperate. The straight line is a linear fit to the data. Inset: time dynamics of the normalized EL intensity excited by square pulses at four different voltages. The formula used in the linear fit is also shown in the inset.

We previously measured the Er excitation cross section at 1535 nm under nonresonant optical excitation at 458 nm (2.71 eV) and showed that the cross section is directly related to the absorption coefficient of the SiN$_x$ material.[16] Moreover, it is known that the absorption cross section of SiN$_x$ increases exponentially at higher energies due to the exponential band-tails formed by localized states in the band gap.[22] We also measured an excitation cross section (for a sample with a similar excess Si) of 1×10^{-16} cm^2 under optical excitation at 2.71 eV,[16] which is less than one order of magnitude compared to the value obtained in this work under electrical excitation of our device structures. Moreover, considering that the electrical excitation occurs at higher energies compared to the optical excitation (the laser energy utilized in photoluminescence was 2.71 eV) one can notice that the two excitation cross sections (optical and electrical) for Er in our material are indeed similar. Additionally, we note that the EL from the Er:SiN$_x$ LEDs was observed only under forward bias as opposed to Er doped crystalline Si (Ref. 23 and some studies on Er doped Si nanocrystals in SiO$_2$ (Ref. 3) where the Er emission was observed under both forward and reverse bias conditions. Finally, the applied electric fields are relatively low in our devices, and the I-V curves can be fitted by the PF emission, preventing hot-carrier generation and the resulting impact ionization mechanism.[17] Based on this discussion, we believe that the EL in our devices is due to PF bipolar injection of electrons (from the ITO electrode) and holes (from the p-type Si substrate) into the Er:SiN$_x$ film, followed by energy transfer to Er ions, analogously to the situation under optical pumping.[16] Additional evidence of this model is provided by the fact that Er:SiN$_x$ devices fabricated on n-type Si substrates did not show any EL under forward and reverse bias (data not shown).

In conclusions, we fabricated Er doped silicon nitride based LEDs operating at voltages as low as 5 V. The LEDs show Er related EL in the visible and in the infrared spectral range. The EL mechanism in our devices can be explained by PF bipolar injection of electron-hole pairs followed by energy transfer to Er ions. We determined that the electrical transport in these devices results from PF injection and we showed that current conduction increases significantly with excess Si in Er:SiN$_x$ films. Finally, we measured the excitation cross section of the Er 1535 nm emission under electrical pumping and we showed that its value is indeed similar to what was observed under optical pumping. Further optimization of Er:SiN$_x$ LEDs is underway to quantify the Er EL efficiency and to enhance it by means of photonic/plasmonic coupling and the fabrication of thin-film superlattice structures with improved transport properties.

[1]L. C. Kimerling, L. Dal Negro, S. Saini, Y. Yi, D. Ahn, S. Akiyama, D. Cannon, J. Liu, J. G. Sandland, D. Sparacin, J. Michel, K. Wada, and M. R. Watts, in *Silicon Photonics*, edited by D. J. Lockwood and L. Pavesi (Springer, New York, 2004).

[2]B. Zheng, J. Michel, F. Y. G. Ren, L. C. Kimerling, D. C. Jacobson, and J. M. Poate, Appl. Phys. Lett. **64**, 2842 (1994).

[3]A. Irrera, F. Iacona, G. Franzo, M. Miritello, R. Lo Savio, M. E. Castagna, S. Coffa, and F. Priolo, J. Appl. Phys. **107**, 054302 (2010).

[4]O. Jambois, F. Gourbilleau, A. J. Kenyon, J. Montserrat, R. Rizk, and B. Garrido, Opt. Express **18**, 2230 (2010).

[5]A. Kanjilal, L. Rebohle, W. Skorupa, and M. Helm, Appl. Phys. Lett. **94**, 101916 (2009).

[6]F. Iacona, D. Pacifici, A. Irrera, M. Miritello, G. Franzo, F. Priolo, D. Sanfilippo, G. Di Stefano, and P. G. Falica, Appl. Phys. Lett. **81**, 3242 (2002).

[7]M. Wang, J. Huang, Z. Yuan, A. Anopchenko, D. Li, D. Yang, and L. Pavesi, J. Appl. Phys. **104**, 083505 (2008).

[8]N. M. Park, T. S. Kim, and S. J. Park, Appl. Phys. Lett. **78**, 2575 (2001).

[9]R. Li, S. Yerci, and L. Dal Negro, Appl. Phys. Lett. **95**, 041111 (2009).

[10]R. Li, J. R. Schneck, J. Warga, L. Ziegler, and L. Dal Negro, Appl. Phys. Lett. **93**, 091119 (2008).

[11]Y. Gong, M. Makarova, S. Yerci, R. Li, M. Stevens, B. Baek, S. W. Nam, L. Dal Negro, and J. Vuckovic, Opt. Express **18**, 13863 (2010).

[12]Y. Gong, M. Makarova, S. Yerci, R. Li, M. Stevens, B. Baek, S. W. Nam, L. Dal Negro, and J. Vuckovic, Opt. Express **18**, 2601 (2010).

[13]A. Gopinath, S. V. Boriskina, S. Yerci, R. Li, and L. Dal Negro, Appl. Phys. Lett. **96**, 071113 (2010).

[14]Y. Gong, S. Yerci, R. Li, L. Dal Negro, and J. Vuckovic, Opt. Express **17**, 20642 (2009).

[15]J. Warga, R. Li, S. N. Basu, and L. Dal Negro, Appl. Phys. Lett. **93**, 151116 (2008).

[16]S. Yerci, R. Li, S. O. Kucheyev, T. van Buuren, S. N. Basu, and L. D. Negro, Appl. Phys. Lett. **95**, 031107 (2009).

[17]O. Jambois, Y. Berencen, K. Hijazi, M. Wojdak, A. J. Kenyon, F. Gourbilleau, R. Rizk, and B. Garrido, J. Appl. Phys. **106**, 063526 (2009).

[18]S. Habermehl and C. Carmignani, Appl. Phys. Lett. **80**, 261 (2002).

[19]We believe that one reason for the higher turn-on voltage for 980 nm peak is the lower quantum efficiency of the detector and the experimental system at 980 nm.

[20]D. Pacifici, G. Franzo, F. Priolo, F. Iacona, and L. Dal Negro, Phys. Rev. B **67**, 245301 (2003).

[21]S. Coffa, G. Franzo, and F. Priolo, Appl. Phys. Lett. **69**, 2077 (1996).

[22]S. Yerci, R. Li, S. O. Kucheyev, T. van Buuren, S. N. Basu, and L. D. Negro, IEEE J. Sel. Top. Quantum Electron. **16**, 114 (2010).

[23]G. Franzò, S. Coffa, F. Priolo, and C. Spinella, J. Appl. Phys. **81**, 2784 (1997).